Structural Engineering and Mechanics, *Vol. 66, No. 3 (2018) 379-386*
DOI: https://doi.org/10.12989/sem.2018.66.3.379

The discrete element method simulation and experimental study of determining the mode I stress-intensity factor

Alireza Bagher Shemirani[1], Hadi Haeri*[2], Vahab Sarfarazi[3], Abbas Akbarpour[4] and Nima Babanouri[3]

[1]Department of Civil Engineering, Sadra Institute of Higher Education, Tehran, Iran
[2]Young Researchers and Elite Club, Bafgh Branch, Islamic Azad University, Bafgh, Iran
[3]Department of Mining Engineering, Hamedan University of Technology, Hamedan, Iran
[4]Department of Civil Engineering, South Tehran Branch, Islamic Azad University, Tehran, Iran

(Received September 14, 2017, Revised January 31, 2018, Accepted February 8, 2018)

Abstract. The present study addresses the direct and indirect methods of determining the mode-I fracture toughness of concrete using experimental tests and particle flow code. The direct method used is compaction tensile test and the indirect methods are notched Brazilian disc test, semi-circular bend specimen test, and hollow center cracked disc. The experiments were carried out to determine which indirect method yields the fracture toughness closer to the one obtained by the direct method. In the numerical analysis, the PFC model was first calibrated with respect to the data obtained from the Brazilian laboratory test. The crack paths observed in the simulated tests were in reasonable accordance with experimental results. The discrete element simulations demonstrated that the macro fractures in the models are caused by microscopic tensile breakages on large numbers of bonded particles. The mode-I fracture toughness in the direct tensile test was smaller than the indirect testing results. The fracture toughness obtained from the SCB test was closer to the direct test results. Hence, the semi-circular bend test is recommended as a proper experiment for determination of mode-I fracture toughness of concrete in the absence of direct tests.

Keywords: fracture toughness; CT; NBD; SCB; HCCD; bonded particle modeling

1. Introduction

Application of fracture mechanics is a topic of interest providing basic knowledge about the behavior of engineering structures. The value of the stress intensity factor which brings the crack to the verge of growth is defined as the mode-I fracture toughness. The concrete fracture toughness controls stability of concrete structures, hence, it is of great importance in various areas such as tunnel excavation, hydraulic-fracturing, and stability analysis of surface and underground rock structures.

The mode-I fracture toughness of concrete can be determined through several standard methods, including the compact tension (CT) test, semi-circular bend (SCB) specimen, short rod (SR) specimen, chevron bend (CB) specimen, cracked chevron notched Brazilian disk (CCNBD) specimen, and hollow center cracked disc (HCCD) (Mahajan and Ravi-Chandar 1989, Maccagno and Knott 1989, He *et al.* 1990, Suresh *et al.* 1990, Singh and Sun 1990, Karfakis and Akram 1993, Lim *et al.* 1993, 1994, Khan and Al-Shayea 2000, Molenaar *et al.* 2002, Chang *et al.* 2002, Sato and Hashida 2006, Obara *et al.* 2007, Kuruppu *et al.* 2010, Dai *et al.* 2010, 2011, 2015, Tutluoglu and Keles 2011, Amrollahi *et al.* 2011, Aliha *et al.* 2012, Kataoka and Obara 2013, Ramadoss and Nagamani 2013, Haeri *et al.* 2013, 2014a, 2014b, 2015a, 2015b, 2015c, 2015d, 2015e, 2015f, 2015g, 2015h, Yu and Lu 2015, Lee *et al.* 2015, Akbas 2016, Rajabi *et al.* 2016, Mosabepranah and Eren 2016, Shemirani *et al*. 2016, 2017, Sarfarazi *et al*. 2017a, b, c, Shemirani *et al*. 2018). The dynamic fracture toughness, describing the behavior of materials under fracturing at high strain rates, is commonly determined using the Hopkinson bar and the drop-weight machine (Guo *et al.* 2011). The International Society for Rock Mechanics (ISRM) suggested the short rod and the chevron bending (CB) tests in 1988 (Zhou *et al.* 2012) and the cracked chevron notched Brazilian disc (CCNBD) in 1995 for determining the rock toughness (Fowell 1995). Tang *et al*. (1990) used cubic-shaped samples to determine the fracture toughness of marbles. Wang *et al*. studied the rock fracture toughness using holed-cracked flattened Brazilian discs and cracked straight-through fattened Brazilian discs (Wang *et al.* 2010, 2011). Morozov et al. measured the stress intensity factor for a number of rock types (Morozov*et al.* 2009). Chen used notched semi-circular bends to determine rock fracture parameters (Chen *et al.* 2009). Die et al. determine the fracture toughness of granites using cracked chevron notched Brazilian disc and notched semi-circular bends (Dai *et al.* 2010, 2011). The core-based tests are often used in studying rock fracture toughness since their samples are easily prepared from natural rocks.

In addition to the experimental studies, a number of numerical analyses of rock fracture behavior have been conducted. Wei et al. simulated the fracture process zone in the ISRM-suggested semi-circular bend rock specimens and chevron notched specimens using the finite element method (Wei *et al.* 2016a, 2016b). Dai *et al*. (2015) numerically investigated the fracture growth in CCNBD specimens. In

∗Corresponding author, Ph.D.
E-mail: h.haeri@bafgh-iau.ac.ir or haerihadi@gmail.com

ISSN: 1225-4568 (Print), 1598-6217 (Online)

another work, the crack propagation in the CCNBD test under mixed mode loading was numerically modeled (Xu *et al.* 2016).

In this paper, fracture behavior of concrete specimens in the NBD, SCB, HCCD, and CT tests was experimentally and numerically studied. First, values of the mode-I fracture toughness were determined through the four suggested experimental methods, and compared together. Then, a particle flow analysis was performed to numerically simulate the fracture propagation. The numerically observed pattern of crack propagation and the obtained values of mode-I fracture toughness demonstrated a good agreement with those of experiments.

2. Experimental tests

2.1 Sample preparation

To avoid the effect of individual difference in the material properties in different tests, samples made of exactly the same material were required. Hence, a concrete specimen was used in this study. Several researchers have used artificial specimens to investigate the influence of crack parameters on the rock-like fracture toughness (Huang *et al.* 2015). The specimens were prepared from a mixture of two parts water, one part fine sand, and two parts cement. Mixing, casting and curing of specimens were carefully controlled to obtain reproducible properties. Mixing the material constituents was carried out with a blender. The most important characteristics of this material are its brittleness and relatively long gelation. However, the material used represents weak rocks.

The methods of NBD, SBC, HCCD, and CT testing were considered in the study, because of their wide application. Fig. 1 schematically shows the above-mentioned methods of fracture toughness testing. The mixed material was cast to prepare the CT, NBD, SCB and HCCD specimens (Fig. 2). Intact samples of the Brazilian test were also prepared for determination of tensile strength of the rock-like material. All samples were kept in laboratory room for 20 days at the temperature of 20 ± 2ºC before being subjected to mechanical testing. The NBD, SCB, HCCD and CT tests were then performed for determining the fracture toughness and failure mode.

2.2 NBD test

The tip of the crack experiences high concentration of stress when an external force is applied to a notched concrete specimen. The pre-existing crack commences propagating provided that the stress concentration reaches a threshold value. After the failure occurred, the fracture toughness is calculated in terms of the stress intensity factor (SIF) which is a function of the failure load, notch size, and other geometrical parameters of the specimen. In this research, a circular disk with a central notch was subjected to vertical compressive load (Fig. 1(a)). The fracture toughness was calculated according to the theoretical relationships, presented by Atkinson *et al*. as follows (Atkinson *et al.* 1982)

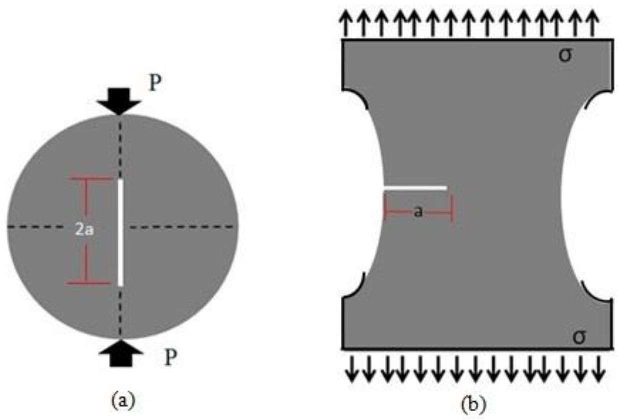

Fig. 1 Schematic view of different methods of fracture toughness testing: (a) NBD specimen under diametrical compression, and (b) Specimen consisted of an edge crack under direct tensile loading

$$KI = \frac{P\sqrt{a}}{\sqrt{\pi R B}} NI \tag{1}$$

$$NI = -3 + 4(a/R)^2 \tag{2}$$

where KI is the mode-I stress intensity factor; R is radius of the Brazilian disk; B is thickness of the disk; P is the compressive load at failure; a is half crack length; and, NI is a non-dimensional coefficient which depends on a/R and the orientation angle (β). The value of KI was calculated to be 1.71 MPa√m using the NBD test.

2.3 SCB test

The SCB test developed by Chong and Kuruppu (1984). The specimens of the SCB testing are cylindrical that do not require any large loading equipment to be tested. The mode-I fracture toughness, KI, is calculated using the following equations (Kuruppu *et al.* 2007)

$$KI = \frac{P\sqrt{\pi a}}{2Rt} YI \tag{3}$$

$$YI = 1.297 + 9.516\left(\frac{s}{2R}\right) - \left(0.47 + 16.457\left(\frac{s}{2R}\right)\right) + \left(1.071 + 34.401\left(\frac{s}{2R}\right)\right)\left(\frac{a}{R}\right)^2 \tag{4}$$

Where a, R, and t are an artificial notch length, radius, and thickness of the specimen, respectively, and P is a maximum load. The normalized stress intensity factor, YI, is dimensionless and given as a function of a dimensionless notch length, a/R, and the ratio of half of the support span to radius s/R. Fig. 2(b) shows the characteristics of the SCB specimen used in this study. A value of 1.65 MPa√m was obtained for KI from the SCB test.

2.4 HCCD test

The HCCD test introduced by Shiryaev and Kotkis

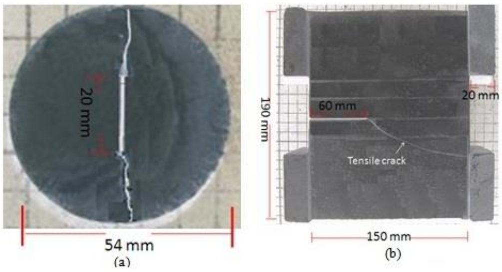

Fig. 2 Failure pattern in, (a) NBD sample and (b) CT test

(1983). As can be seen, the HCCD specimen is a hallow disc of outer radius R_o and inner radius R_i in which two straight central cracks with length of a are created from the inner surface. Change of the crack angle (β) can be resulted in different modes of fracturing. The pure mode-I of fracture occurs for β=0º. The stress intensity factors (KI) in the HCCD specimen is written as below (Shiryaev and Kotkis 1983)

$$KI = \frac{P}{t(Ro - Ri)}\sqrt{\pi a YI} \tag{5}$$

Where P is the applied load and t is the thickness of specimen; YI is the dimensionless stress intensity factors depending on (R_o/R_i), $a/(R_o-R_i)$, and β.

The calibration factor YI for various values of R_i/R_o, a and β were calculated by means of the finite element method. The angle corresponding to pure mode-II depends on R_i/R_o and $a/(R_o-R_i)$. The HCCD test yielded a value of 1.78 MPa√m for KI.

2.5 CT test

The compact tension test is a direct method in which the fracture toughness of materials is determined by applying the tensile load on the crack surface (Fig. 1(b)). The fracture toughness is determined by the following equation (Sato and Hashida 2006)

$$KI = 1.122\sigma\sqrt{\pi a} \tag{6}$$

where KI is the mode -I stress intensity factor, σ is the far field stress at failure, and a is the half-crack length. Fig. 2(b) demonstrates the geometrical characteristics of the CT specimens used. The direct method determined KI to be 1.60 MPa√m.

Fig. 2 shows failure patterns in the different specimens. In all tested samples, the failure mechanism was tensile, since the failure surface was varnished and no pulverized material and no trace of shear displacement was observed. Figs. 2(a) show that in the NBD test tensile cracks initiates from the joint tips propagates parallel to the loading axis until coalesces to the sample edge. In the CT test, tensile cracks initiates from the joint tips, propagates perpendicular to the loading axis until coalesces to the sample edge (Fig. 2(b)).

3. Particle flow analysis

PFC2D is a particle flow code in two dimensions that treats rock-like material as an assemblage of circular disks (Cundall and Strack 1999). The distinct element method is used to model the forces and motions of the particles within the assembly (Cundall and Strack, Potyondy and Cundall 2004). The particles move independently of one another and interact only at contacts. They are assumed to be rigid (non-deformable) but overlap can occur at the contacts. Contacts are assumed to exist only at a point and not over some finite surface area as would be the case with fully deformable particles. The particles can be bonded together to simulate a competent concrete. The contact bonds can be envisaged as a pair of elastic springs (or a point of glue) with constant normal and shear stiffness's acting at a point. The values assigned to this stiffness's influence the macro deformation properties of the concrete sample (Young's modulus and Poisson's ratio). The contact bonds also have a specified shear and tensile strength. The values assigned to these strengths influence the macro strength of the sample and the nature of cracking and failure that occurs during loading. The contact bonds allow tension to exist at the contacts until the force at the contact exceeds the strength of the bond, at which time the bond breaks and the tensile force becomes zero. Similarly, the contact can support shear forces until the bond breaks, but in this case the shear force is set to a residual value that depends on the compressive normal force at the contact and the coefficient of friction. The contact behavior is summarized in Fig. 3. After a bond

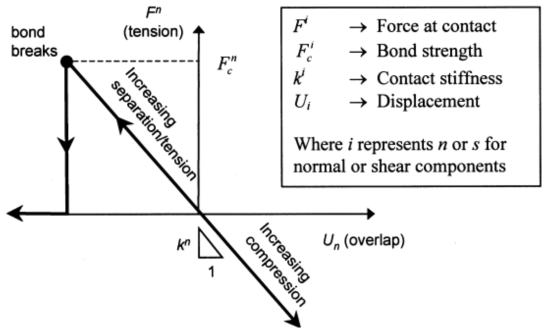

(a)

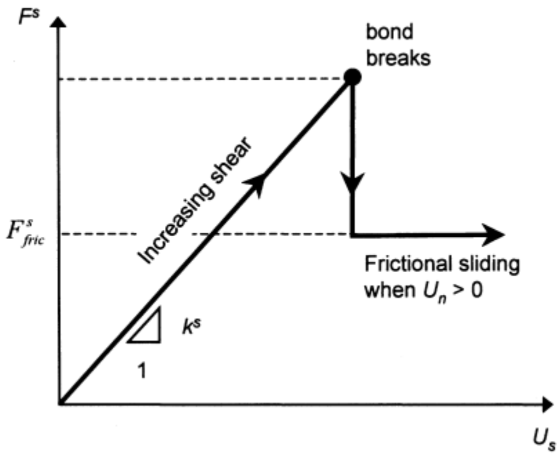

(b)

Fig. 3 Bond behavior under tensile and shear loading: (a) normal component of contact force, and (b) shear component of contact force

Table 1 Micro properties used to represent the physical specimens

Parameter	Value	Parameter	Value
Type of particle	disc	Parallel bond radius multiplier	1
density	3000	Young modulus of parallel bond (GPa)	40
Minimum radius	0.27	Parallel bond stiffness ratio	1.7
Size ratio	1.56	Particle friction coefficient	0.4
Porosity ratio	0.08	Parallel bond normal strength, mean (MPa)	26
Damping coefficient	0.7	Parallel bond normal strength, SD (MPa)	2
Contact young modulus (GPa)	40	Parallel bond shear strength, mean (MPa)	26
Stiffness ratio	1.7	Parallel bond shear strength, SD (MPa)	2


(a)

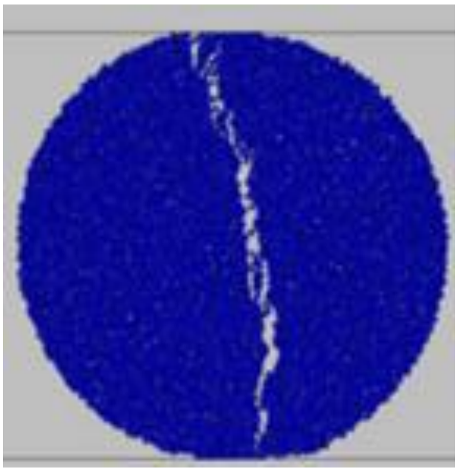
(b)

Fig. 4 Failure pattern in Brazilian testing of intact specimen: (a) physical sample, (b) PFC2D model

breaks in PFC, stress is redistributed and this may then cause more cracks to form nearby. If the concrete model is suitably stressed, then these bond breakages will localize into an inclined macro fracture eventually causing sample failure. In this way, deformation and fracture of concrete specimens are modelled directly by allowing micromechanical damage to evolve, instead of indirectly by using constitutive equations as is the case in most continuum models. It has been shown that PFC can

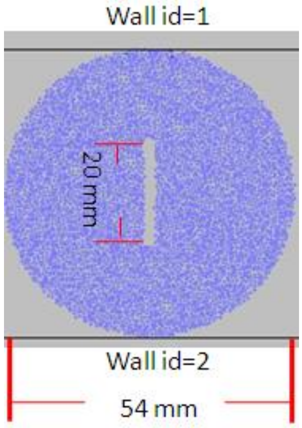

(a)

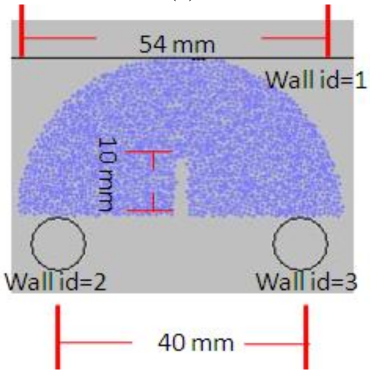

(b)

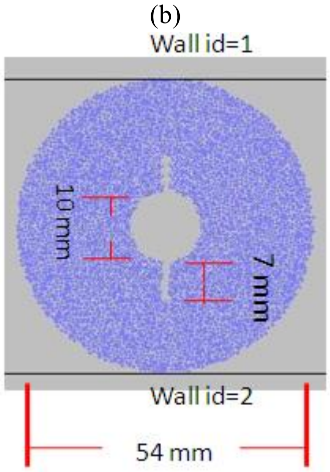

(c)

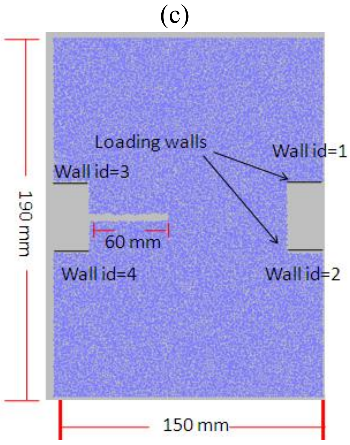

(d)

Fig. 5 Specifications of numerical models: (a) NBD test, (b) SCB test, (c) HCCD test, (d) CT test accurately reproduce the fundamental mechanical behavior of a range of concrete types subjected to different stress regimes (Cundall and Strack 1975).

3.1 Model calibration

The results of the Brazilian test carried out on the intact specimen were used to calibrate the tensile strength of the PFC2D model. Adopting the micro-properties listed in Table 1 and the standard calibration procedures (Potyondy and Cundall 2004), a calibrated PFC particle assembly was created. The diameter of the Brazilian disk considered in the numerical tests was 54 mm. The specimen was made of 5,615 particles. The disk was crushed by the lateral walls moved toward each other with a low speed of 0.016 m/s. The wall velocity was adequately low (0.016 m/s in all tests) to ensure a quasi-static equilibrium. Fig. 4 illustrates the failure patterns of the numerically and experimentally tested samples, respectively. The failure planes experienced in the numerical and laboratory tests are well matching. The values of the tensile strength obtained from the experimental measurement and numerical simulation were 4.6 MPa and 4.5 MPa, respectively, showing a good accordance. The calibrated micro-properties were then used for simulating the fracture toughness tests.

3.2 Simulation of fracture toughness tests

The diameter of the NBD specimen in the numerical modeling was the same considered in the corresponding physical test (i.e., 54 mm). One slit cut with length of 20 mm and opening of 1 mm was created vertically in the center of the model. The specimen was made of 5,015 particles. The disk was crushed by the lateral walls moved toward each other with a low speed of 0.016 m/s. The crack initiation force was registered by taking the reaction forces on the wall 1 in Fig. 5(a).

The SCB test was simulated by creating a semi-circular model in the PFC2D of the calibrated micro-parameters (Fig. 5(b)). Diameter of the model was 54 mm. one slit cut with length of 1 mm and opening of 1 mm was created in lower side of the model. The specimen was made of 2,412 particles. After model preparation, three loading walls were installed in contact with the model. The spacing between the lower walls was 40 mm. The tensile load was applied to the sample by moving the lower and upper walls in the positive and negative y-direction, respectively. The disk was crushed by the loading walls moved toward each other. The force corresponding to the crack initiation was obtained by recording the reaction forces on the wall 1 in Fig. 5(b).

The HCCD test was simulated by creating a circular model in the PFC2D with the calibrated micro-parameters (Fig. 5(c)). Diameter of the ring disk was 54 mm. A circle with diameter of 10 mm was removed from the model center. Two vertical slit cuts with length of 7 mm and opening of 1 mm was created in upper and lower sides of the hole. The specimen was made of 4,312 particles. The disk was crushed by the loading walls moved toward each other.

After calibration of the PFC2D model, the CT test was simulated by creating a model in the PFC2D (Fig. 5(d)).

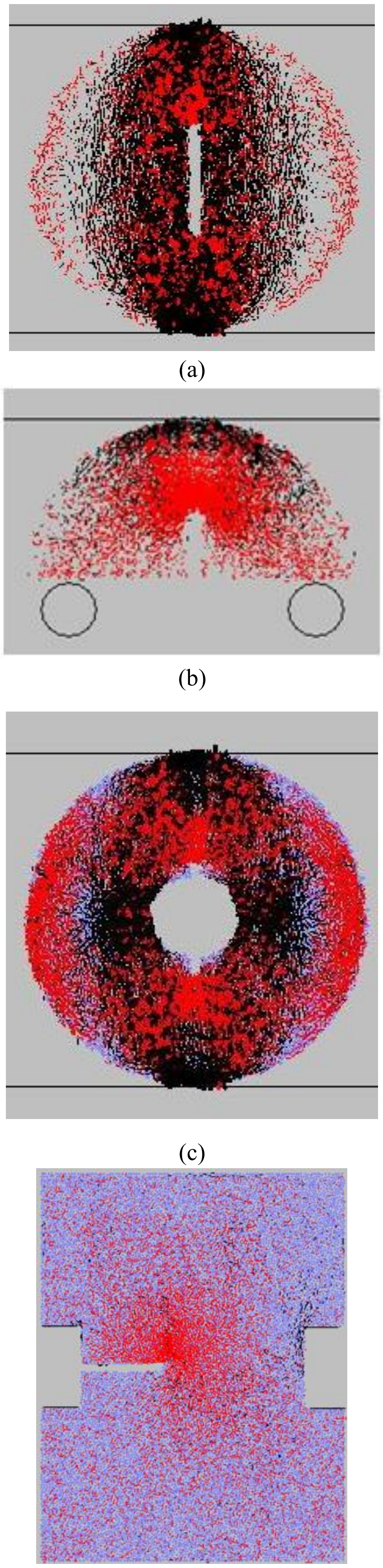

Fig. 6 The distribution of parallel bond forces in the models before the crack initiation occurs; (a) NBD, (b) SCB, (c) HCCD and (d) CT

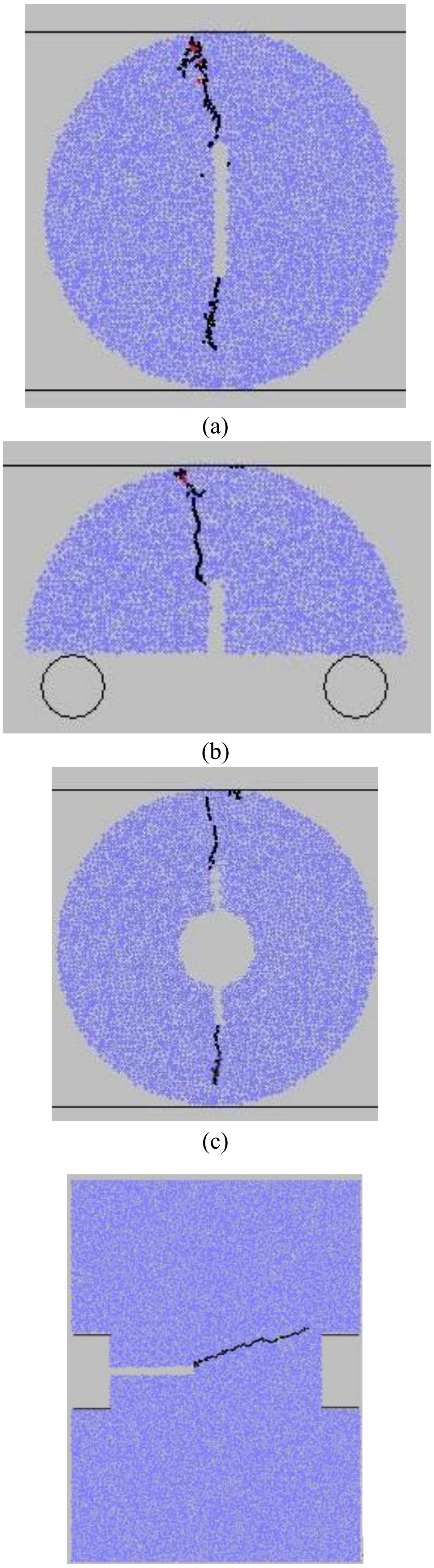

(a)

(b)

(c)

(d)

Fig. 7 Progress of cracks in (a) NBD test, (b) SCB test, (c) HCCD test, and (d) CT test

Table 2 Values of mode-I fracture toughness obtained from different methods

Fracture toughness (MPa√m)	NBD test	SCB test	HCCD test	CT test
Numerical simulation	1.86	1.78	1.91	1.76
Experimental test	1.71			1.60

The PFC specimen had the dimensions of 75 mm×100 mm. A total of 11,179 disks with a minimum radius of 0.27 mm were used to make up the box specimen. Two rectangular zones, with length of 30 mm and thickness of 20 mm, was removed from the right and left sides of the model. After model preparation, four loading walls were installed in contact with upper and lower sides of rectangular zones (Fig. 5(d)). The tensile load was applied to the sample by moving the upper and lower walls in the positive and negative *y*-direction, respectively.

4. Tensile failure mechanism

Fig. 6 shows the parallel bond force distribution at a state before the crack initiation in the four PFC samples. The dark and red lines represent the compression and tensile forces in the model, respectively. The coarser the line is, the larger the force is. As can be seen, the maximum force concentrations occur around the joint tips. In the NBD, SCB and HCCD samples, both of the tensile and compressive forces were distributed in the models (Figs. 6(a), (b) and (c), but the pure tensile force only occurred in the CT test (Fig. 6(d)).

Fig. 7 shows progress of cracks in the simulated fracture toughness tests. Black lines and red lines represent the tensile cracks and shear cracks, respectively. Figs. 7(a), (b) and c show that, in the NBD, SCB and HCCD tests, the tensile crack initiates from the joint tips, propagates parallel to the loading axis until coalesces to the sample edge. In the CT test, the tensile crack propagates perpendicular to the loading axis until coalesces to the sample edge (Fig. 7(d)).

The comparison between Fig. 2 and Fig. 7 shows that the same failure pattern occurred in the numerical models and experimental samples. Table 2 provides a comparison between the values of the mode-I fracture toughness obtained from the NBD, SCB, HCCD, and direct test in both the numerical and experimental studies.

The results show that the values of fracture toughness obtained by the experimental tests were smaller than those obtained by the numerical simulations. The reason is the presence of micro cracks and micro pores in the physical samples which lead to lower fracture toughness. The direct test method (i.e., the CT test) yields the lowest fracture toughness because of applying pure and high tensile stress concentration on the failure surface (Fig. 6(d)). On the other hand, the HCCD test yields the highest fracture toughness values. The difference between the numerical models of the SCB, NBD and HCCD tests with the CT test result was about 2%, 10% and 15%, respectively. It is interesting to note that the fracture toughness value obtained from the SCB test is nearly equal to the CT test result. Therefore, the SCB test can be a proper experiment for determination of fracture toughness of concrete in the absence of direct test.

5. Conclusions

- The failure patterns observed in the experimental studies and numerical modeling were in accordance.
- The particle flow simulations demonstrated that the macro fractures in the models are caused by microscopic tensile breakages on large numbers of bonded discs.
- The mode-I fracture toughness in the direct tensile test was smaller than the indirect test results. The fracture toughness obtained from the SCB test was closer to the direct test results.
- The SCB test can be considered as a proper experiment for determination of the concrete fracture toughness in the absence of direct tests.
- Other advantages shown by the SCB tests are: (1) the test needs less sample size compared with other tests, (2) less material is required for sample preparation, (3) sample preparation is easy, and (4) the use of a simple displacement-controlled compression equipment instead of the complicated apparatus used in other tests.

References

Akbas, S.D. (2016), "Analytical solutions for static bending of edge cracked micro beams", *Struct. Eng. Mech.*, **59**(3), 579-599.

Aliha, M.R.M., Sistaninia, M., Smith, D.J., Pavier, M.J. and Ayatollahi, M.R. (2012), "Geometry effects and statistical analysis of mode I fracture in guiting limestone", *Int. J. Rock Mech. Min. Sci.*, **51**, 128-35.

Amrollahi, H., Baghbanan, A. and Hashemolhosseini, H. (2011), "Measuring fracture toughness of crystalline marbles under modes I and II and mixed mode I-II loading conditions using CCNBD and HCCD specimens", *Int. J. Rock Mech. Min. Sci.*, **48**(7), 1123-1134.

Atkinson, C., Smelser, R.E. and Sanchez, J. (1982), "Combined mode fracture via the cracked Brazilian disk test", *Int. J. Fract.*, **18**(4), 279-291.

Bagher Shemirani, A., Haeri, H., Sarfarazi, V. and Hedayat, A. (2017), "A review paper about experimental investigations on failure behaviour of non-persistent joint", *Geomech. Eng.*, **13**(4), 535-570.

Bagher Shemirani, A., Naghdabadi, R. and Ashrafi, M. (2016), "Experimental and numerical study on choosing proper pulse shapers for testing concrete specimens by split Hopkinson pressure bar apparatus", *Constr. Build. Mater.*, **125**, 326-336.

Bagher Shemirani, A., Sarfarazi, V., Haeri, H., Marji, M. and Hosseini, S. (2018), "A discrete element simulation of a punch-through shear to investigate the confining pressure effects on the shear behaviour of concrete cracks", *Comput. Concrete*, **21**(2), 189-197.

Chang, S.H., Lee, C.I. and Jeon, S. (2002), "Measurement of rock fracture toughness under modes I and II and mixed-mode conditions by using disc-type specimens", *Eng. Geol.*, **66**(1-2), 79-97.

Chen, R., Xia, K., Dai, F., Lu, F. and Luo, S.N. (2009), "Determination of dynamic fracture parameters using a semi-circular bend technique in split Hopkinson pressure bar testing", *Eng. Fract. Mech.*, **76**(9), 1268-1276.

Chong, K. and Kuruppu, M.D. (1984), "New specimen for fracture toughness determination for rock and other materials", *Int. J. Fract.*, **26**(2), R59-62.

Cundall, P.A. and Strack, O.D.L. (1979), "A discrete numerical model for granular assemblies", *Geotech.*, **29**(1), 47-65.

Cundall, P.A. and Strack, O.D.L. (1999), *Particle Flow Code in 2 Dimensions*, Itasca Consulting Group, Inc.

Dai, F., Chen, R., Iqbal, M.J. and Xia, K. (2010a), "Dynamic cracked chevron notched Brazilian disc method for measuring rock fracture parameters", *Int. J. Rock Mech. Min. Sci.*, **47**(4), 606-13.

Dai, F., Wei, M.D., Xu, N.W., Ma, Y. and Yang, D.S. (2015), "Numerical assessment of the progressive rock fracture mechanism of cracked chevron notched Brazilian disc specimens", *Rock Mech. Rock Eng.*, **48**(2), 463-479.

Dai, F., Xia, K., Zheng, H. and Wang, Y.X. (2011), "Determination of dynamic rock mode-I fracture parameters using cracked chevron notched semi-circular bend specimen", *Eng. Fract. Mech.*, **78**(15), 2633-2644.

Fowell, R.J. (1995), "Suggested method for determining mode I fracture toughness using cracked chevron notched Brazilian disc (CCNBD) specimens", *Int. J. Rock Mech. Min. Sci. Geomech. Abstr.*, **32**, 57-64.

Guo, C., Jiang, F., Liu, R. and Yang, Y. (2011), "Size effect on the contact state between fracture specimen and supports in Hopkinson bar loaded fracture test", *Int. J. Fract.*, **169**(1), 77-84.

Haeri, H. (2015g), "Propagation mechanism of neighboring cracks in rock-like cylindrical specimens under uniaxial compression", *J. Min. Sci.*, **51**(3), 487-496.

Haeri, H. (2015h), "Simulating the crack propagation mechanism of pre-cracked concrete specimens under shear loading conditions", *Strength Mater.*, **47**(4), 618-632.

Haeri, H., Khaloo, A. and Marji, M.F. (2015c), "Experimental and numerical simulation of the microcracks coalescence mechanism in rock-like materials", *Strength Mater.*, **47**(1), 740-754.

Haeri, H., Khaloo, A. and Marji, M.F. (2015d), "A coupled experimental and numerical simulation of rock slope joints behavior", *Arab. J. Geosci.*, **8**(9), 7297-7308.

Haeri, H., Khaloo, A. and Marji, M.F. (2015e), "Fracture analyses of different pre-holed concrete specimens under compression", *Acta Mech. Sinic.*, **31**(6), 855-870.

Haeri, H., Khaloo, A. and Marji, M.F. (2015f), "Experimental and numerical analysis of Brazilian discs with multiple parallel cracks", *Arab. J. Geosci.*, **8**(8), 5897-5908.

Haeri, H., Marji, M.F. and Shahriar, K. (2015b), "Simulating the effect of disc erosion in TBM disc cutters by a semi-infinite DDM", *Arab. J. Geosci.*, **8**(6), 3915-3927.

Haeri, H., Shahriar, K., Marji, M.F. and Moarefvand, P. (2013), "Modeling the propagation mechanism of two random micro cracks in rock Samples under uniform tensile loading", *Proceedings of the 13th International Conference on Fracture*, Beijing, China.

Haeri, H., Shahriar, K., Marji, M.F. and Moarefvand, P. (2014a), "On the cracks coalescence mechanism and cracks propagation paths in rock-like specimens containing pre-existing random cracks under compression", *J. Centr. South Univ.*, **21**(6), 2404-2414.

Haeri, H., Shahriar, K., Marji, M.F. and Moarefvand, P. (2014b), "Investigating the fracturing process of rock-like Brazilian discs containing three parallel cracks under compressive line loading", *Strength Mater.*, **46**(3), 133-148.

Haeri, H., Shahriar, K., Marji, M.F. and Moarefvand, P. (2015a), "The HDD analysis of micro cracks initiation, propagation and coalescence in brittle substances", *Arab. J. Geosci.*, **8**(5), 2841-2852.

He, M.Y., Cao, H.C. and Evans, A.G. (1990), "Mixed-mode fracture: The four-point shear specimen", *Acta Metallurg.*

Mater., **38**(5), 839-846.
Huang, Y.H., Yang, S.Q., Tian, W.L., Zeng, W. and Yu, L.Y. (2015), “An experimental study on fracture mechanical behavior of rock-like materials containing two unparallel fissures under uniaxial compression”, *Acta Mech*. *Sinic*., 1-14.

Karfakis, M.G. and Akram, M. (1993), “Effects of chemical solutions on rock fracturing”, *Int*. *J*. *Rock Mech*. *Min*. *Sci*. *Geomech*. *Abstr*., **30**, 1253-1259.

Kataoka, M. and Obara, Y. (2013), “Estimation of fracture toughness of different kinds of rocks under water vapor pressure by SCB test”, *J*. *MMIJ*, **129**, 425-432.

Khan, K. and Al-Shayea, N.A. (2000), “Effect of specimen geometry and testing method on mixed mode I-II fracture toughness of a limestone rock from Saudi Arabia”, *Rock Mech*. *Rock Eng*., **33**(3), 179-206.

Kuruppu, M., Obara, Y. and Kataoka, M. (2010), *Determination of Fracture Toughness of Anisotropic Rocks under Water Vapour Pressure by Semi-Circular Bend Test*.

Kuruppu, M.D., Obara, Y., Ayatollahi, M.R., Chong, K.P. and Funatsu, T. (2013), *ISRM-Suggested Method for Determining the Mode I Static Fracture Toughness Using Semi-Circular Bend Specimen, The ISRM Suggested Methods for Rock Characterization, Testing and Monitoring*, Springer.

Lee, S., Lee, S.H. and Chang, Y.S. (2015), “Evaluation of RPV according to alternative fracture toughness requirements”, *Struct*. *Eng*. *Mech*., **53**(6), 1271-1286.

Lim, I.L., Johnston, I.W. and Choi, S.K. (1993), “Stress intensity factors for semi-circular specimens under three-point bending”, *Eng*. *Fract*. *Mech*., **44**(3), 363-382.

Lim, I.L., Johnston, I.W., Choi, S.K. and Boland, J.N. (1994), “Fracture testing of a soft rock with semi-circular specimens under three-point bending. Part 1-mode I”, *Int*. *J*. *Rock Mech*. *Min*. *Sci*. *Geomech*. *Abstr*., **31**(3), 185-197.

Maccagno, T.M. and Knott, J.F. (1989), “The fracture behaviour of PMMA in mixed modes I and II”, *Eng*. *Fract*. *Mech*., **34**(1), 65-86.

Mahajan, R.V. and Ravi-Chandar, K. (1989), “An experimental investigation of mixed-mode fracture”, *Int*. *J*. *Fract*., **41**(4), 235-252.

Molenaar, A.A.A., Scarpas, A., Liu, X. and Erkens, S. “Semi-circular bending test; simple but useful?”, *J*. *Assoc*. *Asph*. *Pav*. *Technol*., **71**.

Morozov, N., Petrov, Y. and Smirnov, V. (2009), “Dynamic fracture of rocks”, *Proceedings of the 7th EUROMECH Solid Mechanics Conference*, Lisbon, Portugal.

Mosabepranah, M.A. and Eren, O. (2016), “Statistical flexural toughness modeling of ultra high performance concrete using response surface method”, *Comput*. *Concrete*, **17**(4), 477-488.

Obara, Y., Sasaki, K. and Yoshinaga, T. (2007), “Estimation of fracture toughness of rocks under water vapor pressure by semi-circular bend (SCB) test”, *J*. *MMIJ*, **123**(4-5), 145-151.

Potyondy, D.O. and Cundall, P.A. (2004), “A bonded-particle model for rock”, *Int*. *J*. *Rock Mech*. *Min*. *Sci*., **41**, 1329-1364.

Potyondy, D.O., Cundall, P.A. and Lee, C.A. (1996), “Modelling rock using bonded assemblies of circular particles”, *Proceedings of the 2nd North American Rock Mechanics Symposium*, American Rock Mechanics Association.

Rajabi, M., Soltani, N. and Eshraghi, I. (2016), “Effects of temperature dependent material properties on mixed mode crack tip parameters of functionally graded materials”, *Struct*. *Eng*. *Mech*., **58**(2), 217-230.

Ramadoss, P. and Nagamani, K. (2013), “Stress-strain behavior and toughness of high-performance steel fiber reinforced concrete in compression”, *Comput*. *Concrete*, **11**(2), 149-167.

Sarfarazi, V., Haeri, H. and Bagher Shemirani, A. (2017a), “Direct and indirect methods for determination of mode I fracture toughness using PFC2D”, *Comput*. *Concrete*, **20**(1), 39-47.

Sarfarazi, V., Haeri, H., Bagher Shemirani, A. and Zhu, Z. (2017b), “The effect of compression load and rock bridge geometry on the shear mechanism of weak plane”, *Geomech*. *Eng*., **3**(3), 57-63.

Sarfarazi, V., Haeri, H., Bagher Shemirani, A., Hedayat, A. and Hosseini, S. (2017c), “Investigation of ratio of TBM disc spacing to penetration depth in rocks with different tensile strengths using PFC2D”, *Comput*. *Concrete*, **20**(4), 429-437.

Sato, K. and Hashida, T. (2006), “Fracture toughness evaluation based on tension-softening model and its application to hydraulic fracturing”, *Rock Dam*. *Flu*. *Transp*., 1073-1089.

Shiryaev, A.M. and Kotkis, A.M. (1983), “Methods for determining fracture toughness of brittle porous materials”, *Indust Lab*, **48**(9), 917-918.

Singh, R.N. and Sun, G. (1990), “A numerical and experimental investigation for determining fracture toughness of Welsh limestone”, *Min*. *Sci*. *Technol*., **10**(1), 61-70.

Suresh, S., Shih, C.F., Morrone, A. and O’Dowd, N.P. (1990), “Mixed mode fracture toughness of ceramic materials”, *J*. *Am*. *Ceram*. *Soc*., **73**(5), 1257-1267.

Tang, C. and Xu, X. (1990), “A new method for measuring dynamic fracture toughness of rock”, *Eng*. *Fract*. *Mech*., **35**(4-5), 783-791.

Tutluoglu, L. and Keles, C. (2011), “Mode I fracture toughness determination with straight notched disk bending method”, *Int*. *J*. *Rock Mech*. *Min*. *Sci*., **48**(8), 1248-1261.

Wang, Q.Z., Feng, F., Ni, M. and Gou, X.P. (2011), “Measurement of mode I and mode II rock dynamic fracture toughness with cracked straight through flattened Brazilian disc impacted by split Hopkinson pressure bar”, *Eng*. *Fract*. *Mech*., **78**(12), 2455-2469.

Wang, Q.Z., Zhang, S. and Xie, H.P. (2010), “Rock dynamic fracture toughness tested with holed-cracked flattened Brazilian discs diametrically impacted by SHPB and its size effect”, *Experiment*. *Mech*., **50**(7), 877-885.

Wei, M.D., Dai, F., Xu, N.W. and Zhao, T. (2016), “Stress intensity factors and fracture process zones of ISRM-suggested chevron notched specimens for mode I fracture toughness testing of rocks”, *Eng*. *Fract*. *Mech*., **168**, 174-189.

Wei, M.D., Dai, F., Xu, N.W., Zhao, T. and Xia, K.W. (2016), “Experimental and numerical study on the fracture process zone and fracture toughness determination for ISRM-suggested semi-circular bend rock specimen”, *Eng*. *Fract*. *Mech*., **154**, 43-56.

Xu, N.W., Dai, F., Wei, M.D., Xu, Y. and Zhao, T. (2016), “Numerical observation of three dimensional wing cracking of cracked chevron notched Brazilian disc rock specimen subjected to mixed mode loading”, Rock Mech. *Rock Eng*., **49**(1), 79-96.

Yu, K. and Lu, Z. (2015), “Influence of softening curves on the residual fracture toughness of post-fire normal-strength concrete”, *Comput*. *Concrete*, **15**(2), 199-213.

Zhou, Y.X., Xia, K., Li, X.B., Li, H.B., Ma, G.W., Zhao, J., Zhou, J.L. and Dai, F. (2012), “Suggested methods for determining the dynamic strength parameters and mode-I fracture toughness of rock materials”, *Int*. *J*. *Rock Mech*. *Min*. *Sci*., **49**, 105-112.

CC